



## PV/T Performance Evaluation as Electricity Generation and Hot Air Supplier for Fully and Partially Covered with PV Modules

Jalal M. Jalil <sup>a</sup>, Ahmed A. Hussein <sup>b</sup>, Anwar J. Faisal <sup>c</sup>

<sup>a</sup> Electromechanical Engineering Department, University of Technology-Iraq. [jalalmjalil@gmail.com](mailto:jalalmjalil@gmail.com)

<sup>b</sup> Electromechanical Engineering Department, University of Technology-Iraq. [ahmedabdulgaderhussein@gmail.com](mailto:ahmedabdulgaderhussein@gmail.com)

<sup>c</sup> Electromechanical Engineering Department, University of Technology-Iraq. [anwarjabarfaisal@gmail.com](mailto:anwarjabarfaisal@gmail.com)

\* Corresponding author

Submitted: 4/09/2019

Accepted: 30/10/2019

Published: 25/07/2020

### KEY WORDS

PV/T system, PV modules temperature, PV efficiency, Thermal efficiency, Renewable energy, PV/T partially covered with PV.

### ABSTRACT

*The solar energy system is environmentally friendly and the utilization of photovoltaic thermal collectors, (PV/T) has attracted more attention, which directly converts solar radiation into electricity and thermal energy simultaneously. This study investigated the air biased Photovoltaic thermal hybrid solar collectors, (PV/T) trend for two cases, denominate case one (PV/T system fully covered with PV modules), and case tow (PV/T system partially covered with glass). The studied parameters were solar irradiance and the air mass flow rate. The investigation has been performed in terms of outlet air temperature, electrical power, thermal and electrical efficiencies. A numerical model was developed using the computational fluid dynamic program (CFD) and the results were compared with the experimental measurements that carried out from indoor conditions using a solar simulator. A good agreement has been achieved between experimental and numerical results. The performance of both cases one and case two concluded that the PV/T system should be operating at a moderate air flow rate of 0.013 kg/s, which is the best mass flow rate. In addition, it has been observed that for case tow the maximum outlet air temperature and electric powers were 44.3 oC and 26.6 W, respectively. For case one, thermal and electrical efficiencies were found 34% and 10%, respectively, based on the experimental data, while for case 2, the maximum thermal and electrical efficiencies were found to be 48.9 and 9.1%, respectively.*

**How to cite this article:** J. M. Jalil, A. A. Hussein, and A. J. Faisal, "PV/T performance evaluation as electricity generation and hot air supplier for fully and partially covered with PV modules," Engineering and Technology Journal, Vol. 38, Part A, No. 07, pp. 1001-1015, 2020.

DOI: <https://doi.org/10.30684/etj.v38i7A.559>

This is an open access article under the CC BY 4.0 license <http://creativecommons.org/licenses/by/4.0>

## 1. Introduction

PV/T systems are one of the most popular renewable energy resources that face the energy crisis, which is all around the world. It has indicated to the combination of photovoltaic technologies with solar thermal into one single system. The design of photovoltaic thermal (PV/T) was firstly implemented by Kern and Russell [1]. It allows to utilize the solar radiation efficiently and reduces the usage of expensive fossil fuel consumed by converting the solar energy into electrical and thermal energy. Solar energy is available and clean and the use of it decrease the cost of power generation. In addition, the use of solar energy deducts a large portion of carbon dioxide emitted to the environment by burning of fossil fuel [2]. PV system can convert 6-16% of solar incidence into electricity at 25 °C, the remaining 80% of this incident is converted to heat this heat act as losses dissipated to the environment [3]. The heat dissipation is not desirable and can be converted into useful energy such as forced air or water circulation with the backside of the PV surface. Many experiences and researches on different types of solar PV/T collectors had been studied, to analyze the behavior of the PV/T system and factors affected on it, such as various types of working fluid and various design of the fluid flowing channel. Farshchimonfared et al. [4] Experienced the behavior of air biased (PV/T) collectors attached to the Residential buildings under the effect of air mass flow rate, the diameter of air duct and channel depth. The result showed that the optimum value of the mass flow rate per unit area of the collector is approximately equal to 0.021 kg/s.m<sup>2</sup>. In addition, the optimum duct diameter is varying between 0.3 and 0.56 m. Moreover, the optimum channel depth is varied between 0.09 and 0.026 m and this range is increase as the collector area and the ratio of large to width increase. Bambrook and Sproul [5] Developed a circuit simulation program for the air biased PV/T system so as to calculate PV cell temperature, fluid temperature, and the rate of heat transfer along the collector length. The simulation program also provides a method for analyzing the PV/T collector under any dimension and different mass flow rates. They showed that the range of PV cell temperature from inlet to the outlet is about 37 to 53 °C and outlet fluid temperature is 49 °C. Shahsavari and Ameri [6] Tested two, four, and eight fans to investigate the maximum electrical efficiency of the direct-coupled PV/T air collector with glass and without glass cover. The results carried out at the climate condition in Kerman Iran showed that the mass flow rate increase with an increase in the number of fans, therefore the system has the most air flow rate and maximum electrical efficiency when the operation is with eight fans. In addition, the result reveals thermal efficiency, increase when adding glass cover to the PV panel reach 60% but electrical efficiency decreases to 8.5%. Yazdanifard et al. [7] Analyzed the performance of water-based PV/T collectors in laminar and turbulent flow regimes. They showed that the laminar regime has higher PV and outlet fluid temperatures than that for turbulent flow. The PV cell temperature of laminar flow was 39 °C for the glazed system and 36 °C for unglazed one. For turbulent flow, the PV cell temperature for the glazed and unglazed system were 30 and 29 °C respectively. For laminar flow outlet fluid temperature was 31.5 °C for the glazed system and 30 °C for unglazed one. In the case of turbulent flow outlet, fluid temperature for the glazed and unglazed system were 26.3 and 26 °C respectively. Turbulent flow has higher electrical efficiency than that of the laminar regime due to the reduction in PV module temperature. Shuang et al. [8] have designed a numerical model for water biased PV/T systems with a cooling channel above the PV panel to study the electrical and thermal performance when the water channel above the PV panel. The result showed that electrical production decrease, but higher thermal production was presented. There was a 1.2% reduction in electrical efficiency when the cooling channel height increases from 3 to 14 mm. Moreover, the thermal efficiency was increased significantly with the increment of cooling channel height. Tiwari et al. [9] Studied the influence of photovoltaic thermal collector PV/T partially covered with PV modules for water distillation in the climate condition of New Delhi. The system consists of a DC pump for circulating water, partially covered PV/T and solar still, it was seen that the maximum hourly thermal efficiency was 50% and the system can meet the demand of DC electric power and potable water. Tiwari et al. [10] have designed and fabricated a photovoltaic thermal system for a greenhouse, the experiment has been done on the climatic condition of IIT Delhi, India. The variables under study were the effect of packing factor, absorptivity (degradation effect), the mass flow rate of air, and transmissivity (dusting effect) on the system performance. Tonui and Tripanagnostopoulos [11] Studied the cooling of PV/T by natural convection using the air flows through a slim mineral sheet or fins hanging at the mid-side attached to the back surface of air-channel to enhance heat transfer from PV cell to the air stream. The work improves that the system efficiency for every parameter evaluated with the fin

system giving better performance than the thin metal sheet system, but both enhancing the heat transfer from PV module whereas the maximum outlet air temperatures for fin system was 58 and 60 °C for thin metal sheet system.

It can be seen from the previous studies that the researchers attempted to increase electricity and thermal efficiencies by different methods. This work will produce electrical and thermal optimization for air biased PV/T collectors fully covered with PV modules and partially covered with glass and investigate the specific flow rate and optimum area coverage rate of glass that combination with PV modules.

## 2. System Description

Figure 1.a illustrates a schematic diagram of the experimental rig, which mainly consists of four PV panels attached to the aluminum absorber plate, each two of these PV modules have the same size and the same technical data. The detailed description and dimensions of each type of PV solar cell specification is illustrated in Table 1. DC voltage regulator was used to control the flow rate. Solar simulator with microcontroller to control the amount of irradiance, sensors, and measuring Units. Seven units of 500-watt, 220 volts. Halogen lamps is connected on the solar simulator with built-in reflector, the distance between halogen lamps and PV panels is 65 cm, and the distance between the middle of one halogen lamp bulb and the center of another halogen lamp bulb is about 20 cm, in order to cover the whole area of PV modules. Other important components such as solar charger controller and battery are used for power storage. Air is the working medium and supplied to the thermal channel by three DC fans each of 3 W capacity are used to supply the air at a different mass flow rate. The experiment was situated indoor to eliminate the effect of ambient temperature and solar intensity. The adopted PV modules consist of layers in order of glass, Ethylene-Vinyl Acetate (EVA), solar cells, Ethylene-Vinyl Acetate (EVA), and Tedlar. The PV panels are connected in parallel for getting high current and constant voltage and then fixed into the aluminum frame to cover all the PV/T collector which is case 1 (collector fully covered with PV modules) as shown in Figure 1.b Glass cover with dimensions of 0.47 m length, 0.35 m width, and thickness of 3mm is utilized in this work to cover the non-packing area in the case2 (PV/T partially covered with glass).

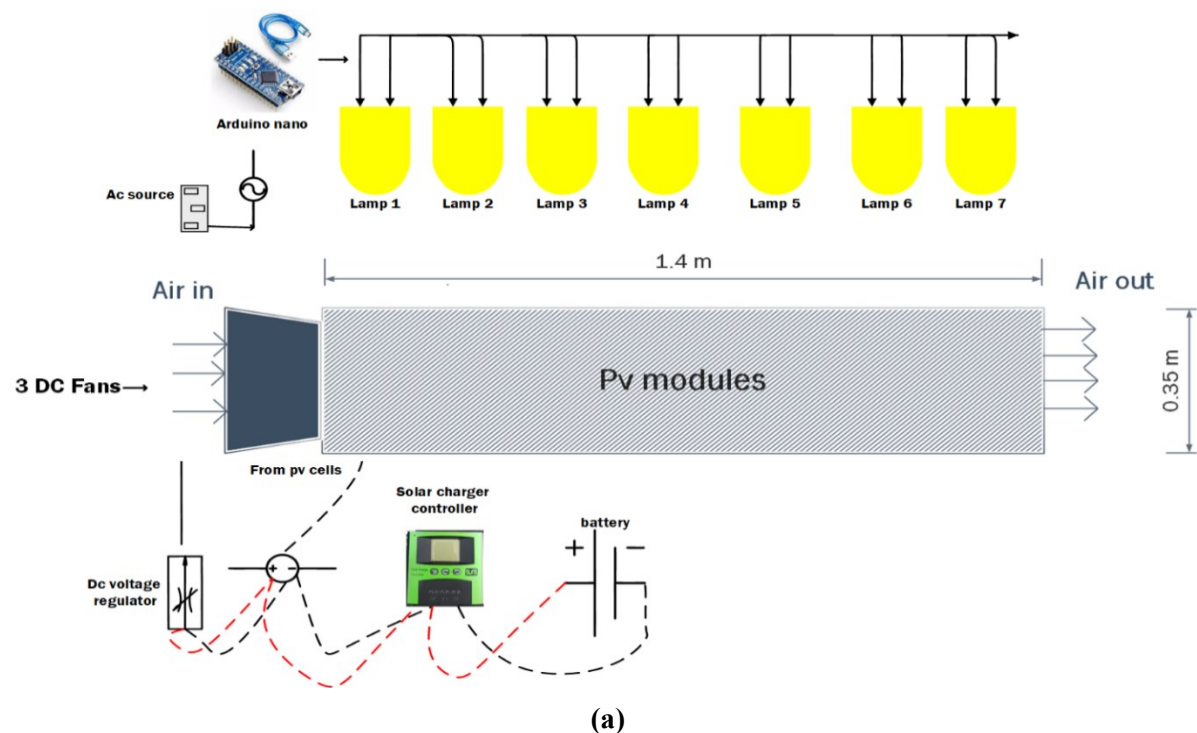




**Figure 1: Air biased PV/T collector, (a) - Sketch of the experimental rig, (b) - Photograph for PV/T system**

The rectangular flat plate collector is constructed from aluminum with dimensions of 1.4 m length, 0.35 m width, and 1 mm thickness is used as a heat absorber from the PV modules. The black matt painted plate is enclosing the PV modules from the sides and bottom to make a channel of 0.03 cm high for air passage. The channel connected to the aluminum frame, which fixed the PV modules with; prevent any air leakage, this connection increases the heat transferred from PV modules to the absorber plat. The polyurethane foam of 3 cm thickness was used to insulate the outer surface of the flat plate collector in order to reduce the heat losses.

**Table 1: Specification of PV modules.**

Group no.	1	2
No. of PV modules	Two (20 watt) PV panels	Two (10 watt) PV panels
Dimensions	47*35 cm <sup>2</sup>	23.5* 35 cm <sup>2</sup>
Current at Pmax	1.1 Amp.	0.57 Amp.
Voltage at P max	17.5 V	17.5 V
Open circuit voltage (Voc)	20 V	20 V
Short circuit current (Ish)	1.2 Amp.	0.64 Amp.

### 3. Experimental Aspects

#### I. Thermal power and collector efficiency

The useful heat gain by air biased on PV/T collector can be calculated using Eq. (1).

$$Q_u = \dot{m} c_p (T_o - T_i) \quad (1)$$

The thermal efficiency can be evaluated using:

$$\eta_{th} = \dot{m} c_p (T_o - T_i) / G A_c \quad (2)$$

Where  $Q_u$  is useful to heat gain from the collector,  $T_o$  and  $T_i$  are the outlet and inlet temperatures of the heat transfer fluid,  $A_c$  is the area of PV/T collector and  $G$  is the irradiance on the collector surface.

#### II. Electrical power and electrical efficiency

The highest power generation and PV efficiency provided in Eqs. (3) and (4). The main parameters used to describe the power are the short circuit current ( $I_{sc}$ ), open-circuit voltage ( $V_{oc}$ ), and the fill factor (FF), which described as the proportion of the maximum power output from the solar cell to the product of  $V_{oc}$  and  $I_{sc}$ .

$$P_e = V_{oc} I_{sc} FF \quad (3)$$

$$\eta_e = P_e / G A_{pv} \quad (4)$$

Where  $\eta_e$  is electrical efficiency,  $P_e$  electrical power output,  $A_{pv}$  is the PV modules area.

#### 4. Numerical Modeling

This study includes mathematical formulation, which governs partial differential equations (PDEs) to depict turbulent fluid flow field and heat transfer in a PV/T system. Two cases of air biased PV/T system have been simulated which are, case 1 (PV/T system fully covered with PV module) and Case 2 (PV/T system partially covered with PV module). Figure 2 reveals the top view of two cases simulated with flow directions. The hybrid PV/T system, which studied numerically, has a full scale of the experimental duct. The duct has 0.35 m width and 1.4 m length. The cross-section of the duct is  $(0.35 * 0.03) m^2$ . A mesh size of  $(62 * 22 * 22)$  elements involved in the numerical solution of the PV/T system. Numerical output characteristics of the PV/T performance are simulated by using FORTRAN 90, and the results are plotted using the Tec plot.

The mathematical model of the airflow is governed by basic conservation of momentum, mass, and energy balance equations. Turbulent flow is considered in the present work (the Reynolds number value of the air inlet is 6133).

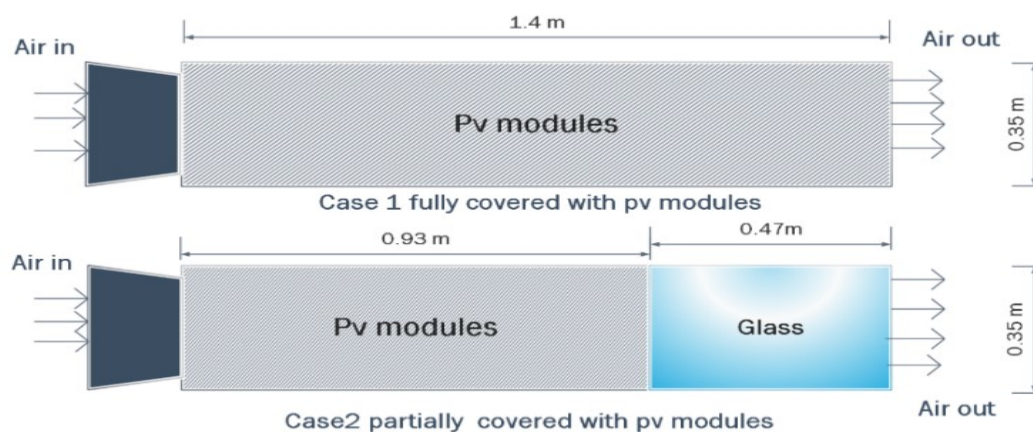


**Figure 2: Top view of two cases simulated with flow directions.**

The following assumptions have been considered:

- i. Steady-state with negligible side and bottom losses, body forces, and air leakage.
- ii. Conservation equation of the three-dimensional model.
- iv. Forced convection of operation and the streamline of air through the duct is uniform.
- v. Three-dimensional heat transfer conduction through PV modules, glass, and absorber plate.
- vi. Turbulent airflow has been considered in the channel.

##### I. Governing Equations

The flow of air inside the PV/T system is turbulent with, 3-D, incompressible, and steady-state. Navier Stokes equations (NSEs) (continuity, momentum, and energy) are resolved by control volume (CV) in Cartesian Coordinates.  $k$ - $\epsilon$  Model is used to simulate the turbulent flow numerically. This model has a couple of equations, which join between turbulent kinetic energy ( $k$ ) equation and turbulence dissipation rate ( $\epsilon$ ) equation.

##### II. Thermal Analysis of Solid Walls

###### PV Modules

Semi-transparent PV modules generate electricity power when the solar cell absorbs the irradiance, also it produces thermal energy from the convection heat transfer between the back wall of PV modules and air flowing. The energy balance for a node (3) of PV modules is shown in Fig. (3) which exhibit a 3-D control volume (CV) the grid point (3) is connected to six contiguous points, identifies as N, S, E, W, N, S corresponding to the north, south, east, west, bottom and top directions. The energy balance for the node (3) of PV modules has been written as follows:

$$q_e + q_w + q_t + q_b + q_n + q_s + q_{flux} = 0 \quad (5)$$

The terms  $q_e$ ,  $q_w$ ,  $q_t$ ,  $q_b$ ,  $q_n$ ,  $q_s$  are the heat transferred to the east, west, top, bottom, north and south of the node respectively which are giving by [13]

$$q_e = k_{PV}A_x \frac{\partial T}{\partial x} = \frac{k_{PV}A_x}{\Delta x} (T_{pv}(i, j, k) - T_{pv}(i + 1, j, k)) \quad (6)$$

$$q_w = k_{PV}A_x \frac{\partial T}{\partial x} = \frac{k_{PV}A_x}{\Delta x} (T_{pv}(i, j, k) - T_{pv}(i - 1, j, k)) \quad (7)$$

$$q_t = k_{PV}A_z \frac{\partial T}{\partial z} = \frac{k_{PV}A_z}{\Delta z} (T_{pv}(i, j, k) - T_{pv}(i, j, k + 1)) \quad (8)$$

$$q_b = k_{PV}A_z \frac{\partial T}{\partial z} = \frac{k_{PV}A_z}{\Delta z} (T_{pv}(i, j, k) - T_{pv}(i, j, k - 1)) \quad (9)$$

$$q_n = q_{conv}(pv\_amb) = h_{out} A_y (T_{pv}(i, j, k) - T_{amb}) \quad (10)$$

$$q_s = k_{PV}A_y \frac{\partial T}{\partial y} = \frac{k_{PV}A_y}{\Delta y} (T_{pv}(i, j, k) - T_{pv}(i, j - 1, k)) \quad (11)$$

$q_{conv}(pv - amb)$  Are the heat losses transferred by convection from PV modules to ambient [13]? Convection is associated with external surfaces, and conduction is performed through the wall of the PV/T collector.

$h_{out}$  is a coefficient of the heat transferred by convection between PV modules or glass surface and the ambient which was given by [14]:

$$h_{out} = 5.7 + 3.8 v_w \quad (12)$$

Where  $v_w$  is the wind velocity.

$q_{flux}$  is the solar radiation absorbed by glass, which can be calculated by [15]:

$$q_{flux} = \alpha_{pv} \tau_g A_y G \quad (13)$$

For the portion covered with PV panels.

$$\text{And } q_{flux} = \tau_g A_y G \quad (14)$$

For the portion covered with glass cover, where  $\alpha_{pv}$  is PV modules absorptivity and equal 0.9 [16] and  $\tau_g$  is the glass transmittance and equal 0.9 [17].

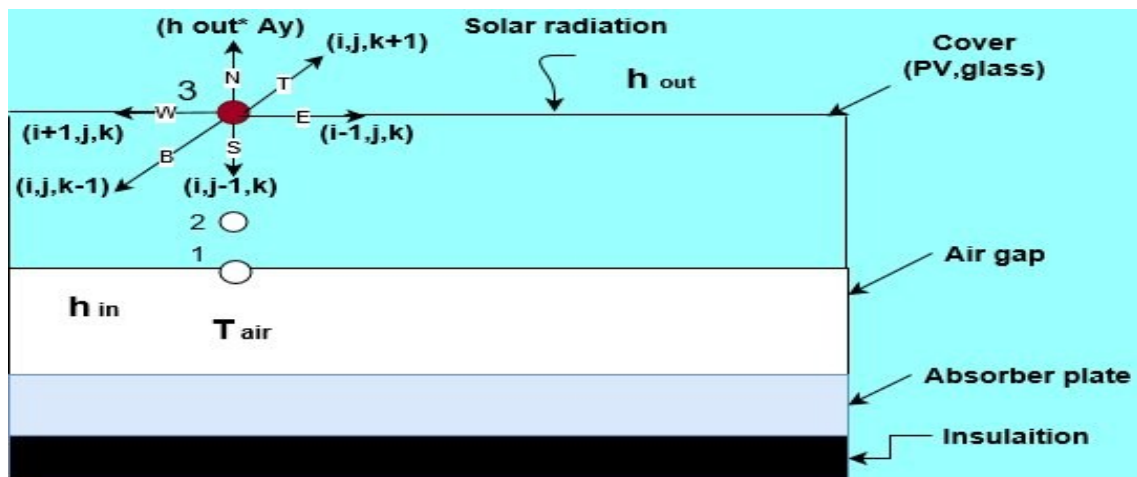


Figure 3: The energy balance for the node (3) of PV modules.

The composite thermal conductivity through the PV module  $k_{pv}$  is determined using Eq. (20) [1^].

$$k_{pv} = \frac{\delta_{tot}}{\frac{\delta_{eva}}{k_{eva}} + \frac{\delta_{ted}}{k_{ted}} + \frac{\delta_{sc}}{k_{sc}} + \frac{\delta_g}{k_g}} \quad (15)$$

$\delta$  Is denote the thickness and  $k$  is the thermal conductivity.

$$A_x = \Delta y \Delta z$$

$$A_y = \Delta x \Delta z$$

$$A_z = \Delta x \Delta y$$

Suppose

$$a_e = a_w = \frac{k_{pv}A_x}{\Delta x}, a_t = a_b = \frac{k_{pv}A_z}{\Delta z}, a_s = \frac{k_{pv}A_y}{\Delta y}, a_n = h_{out}A_y$$

$$a_p = a_e + a_w + a_t + a_b + a_n + a_s$$

After substituting these terms in Eq. (5) it becomes:

$$T_{pv(I,J,K)} = \left[ a_e T_{pv(i+1,j,k)} + a_w T_{pv(i-1,j,k)} + a_t T_{pv(i,j,k+1)} + a_b T_{(i,j,k-1)} + a_n * T_{amb+a_s T_{(i,j-1,k)}+a_e * q_{flux}} \right] / a_p \quad (16)$$

The temperature of any point of PV cells can be calculated by Eq. (16)

## 5. Results and Discussion

The presentation and debate of experimental and numerical outcomes of hybrid photovoltaic thermal PV/T air collectors are discussed in this section. The experiments are carried out for the two cases of PV/T air collector, Figures 4,5 and 6 show the air, PV cell, and absorber plate temperature respectively along with the distance of PV/T collector for case 1 at different values of flow rate and 800 w/m<sup>2</sup> solar radiation. From figures, it is observed that the temperatures increase with mass flowrate decrease due to a small amount of heat is extracted at low flowrate. Therefore, the maximum temperature for air, PV cell, and plate are 37 °C, 65°C and 40 °C respectively recorded at 0.0098 kg/s flow rate. High solar radiation increases the intensity of the electric field and thus the voltage increase, for these reasons the electric power increases as shown in Figure 7. From this figure one can observe that the maximum output power was found 40.8W at high flowrate 0.016 kg/s and 1000 W/m<sup>2</sup> and the minimum output power was found 10.2 W at low flowrate 0.0098 kg/s and 400 W/m<sup>2</sup>. For heat transfer, high fluid flowrate means low air temperature difference between inlet and outlet but the high heat transfer rate reached 168.84 W as reveals in Figure 8.

To analyze the efficiency of PV/T fully covered with PV Figures 9 and 10 show the electrical and thermal efficiency respectively, one can observe from these figures that rising the flow rate leads to a positive effect on the electrical and thermal efficiencies, because of high flow rate lead to high heat extracted by air from PV modules, this means high power generated by PV modules. Therefore, the maximum electrical and thermal efficiency was found 10% and 34% respectively at 0.016kg/s flow rate. In order to reach the balance in electrical and thermal output Figure 11 plots the variation of electrical and thermal output depending on the variation of flow rate at constant irradiance and ambient temperature. It is clear from the figure that the PV/T collector should be operated at the moderate flowrate (0.013 kg/s) to produce high electrical and thermal output reached 22.5 W electrical power and 32 °C the outlet air temperature. For case two, 0.33% of the PV/T area is covered with glass at the outlet portion. Figure 12 reveals the variation of air temperature along with the distance of the PV/T system at different values of irradiance. Figure 13 illustrates the variation of absorber plate temperature along with the distance of the PV/T system at different values of irradiance. Figure 14 shows the variation of (PV cell and glass) temperature along with the distance of the PV/T system at different values of irradiance. It was observed from Figure 12 that the maximum outlet air temperature was 44.3 °C obtained at 1000W/m<sup>2</sup> and this sharp increase in outlet air temperature is due to the direct radiation fall into the glass at outlet portion and restricts the heat gain in this position without making this radiation to passing parallel with PV modules. From Figure 13, one can observe that the optimum rising in absorber plate temperature reached 60 °C due to the existence of glass above it at the outlet portion. The PV modules have higher temperatures for the case of partially covered with glass than the case of fully covered as shown in Figure 15. Additionally, the reduction in the area of PV cell leads to a reduction in electric power generated also, which is depicted in Figure 15. It is observed from Figures 16 and 17 the variation of electrical and thermal efficiencies respectively with the variation of the area covered by PV modules at a different mass flow rate. The result reveals that thermal efficiency significantly reaches to 55% in the area of glass increase to the half area of collector for high flow rate. Conversely, the electrical energy decreases as the area covered by the PV module decrease, in this case, the PV module area should be optimized to satisfy the electrical power required for DC fans. In contours Figures, the three-dimensional plot for PV cell is plotted at an airflow of 0.013 kg/s. Figures 18 and 19 show isotherm contours of PV cell for case1 (fully-covered with PV) and case 2 (partially covered with glass at outlet portion) respectively. The graph shows that higher temperature was obtained in case of partially covered with glass due to receiving solar radiation from two direction, first, the irradiance falls directly on it and second the radiation from a non-packing area with PV modules. The PV modules, plate and air temperatures obtained by Experimental work has been compared with the numerical results and plot in Figure 20 for the case 1 (fully covered with PV modules) and Figure 21 for case 2 (partially covered with glass at outlet portion). These figures showed strong agreement has been achieved between the experimental and numerical outcomes.

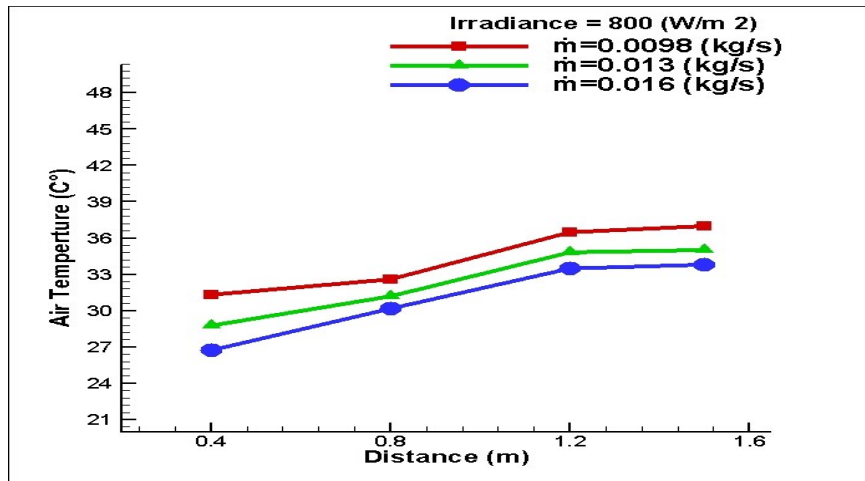


Figure 4: The experimental air temperature variation along with the distance of the PV/T collector in case 1 (fully covered with PV) at different flow rate.

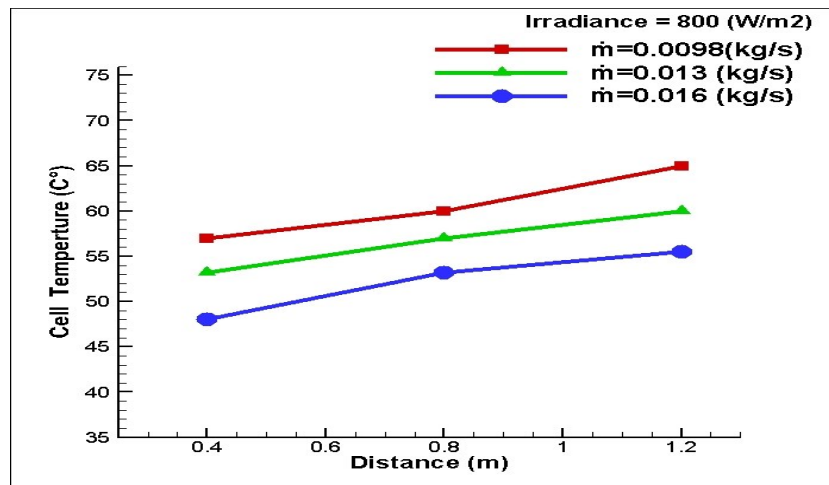


Figure 5: The experimental PV cell temperature variation along with the distance of the PV/T collector in case 1 (fully covered with PV) at a different flow rate

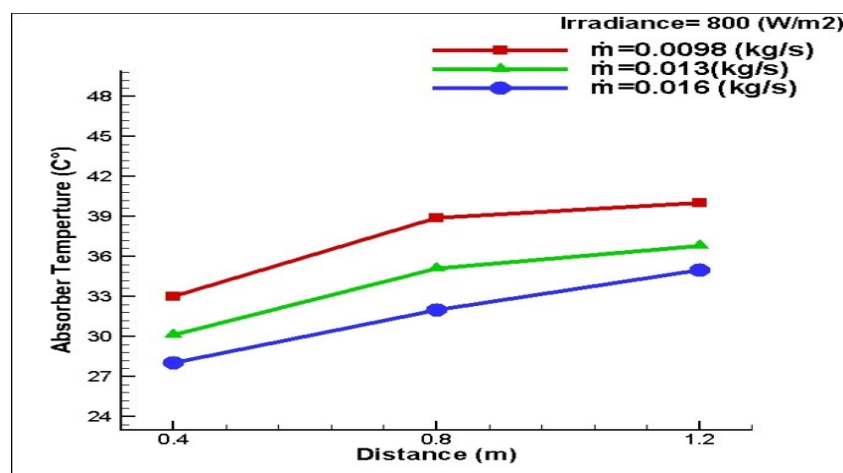


Figure 6: The experimental absorber plate temperature variation along with the distance of the PV/T collector in case 1 (fully covered with PV) at a different flow rate.

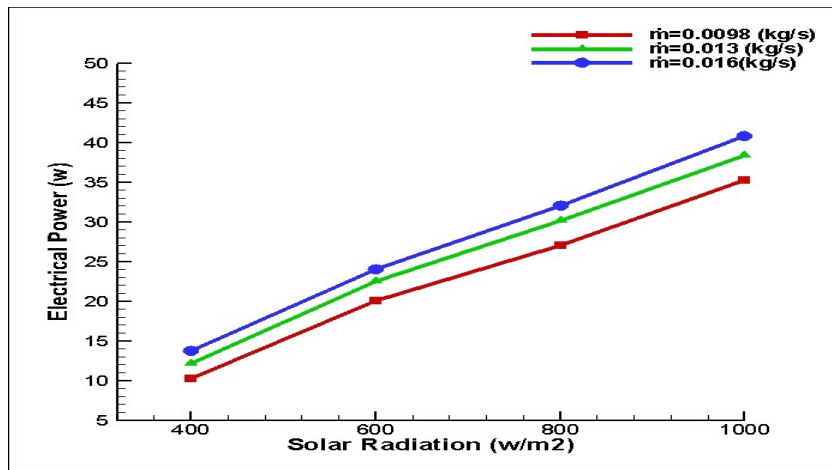


Figure 7: The experimental variation of electrical power in case 1 (fully covered with PV) at a different flow rate.

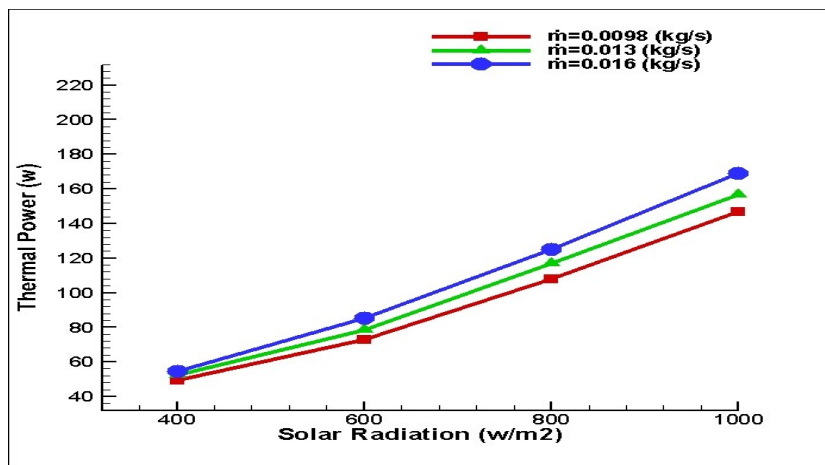


Figure 8: The experimental variation of thermal power in case 1 (fully covered with PV) at a different flow rate.

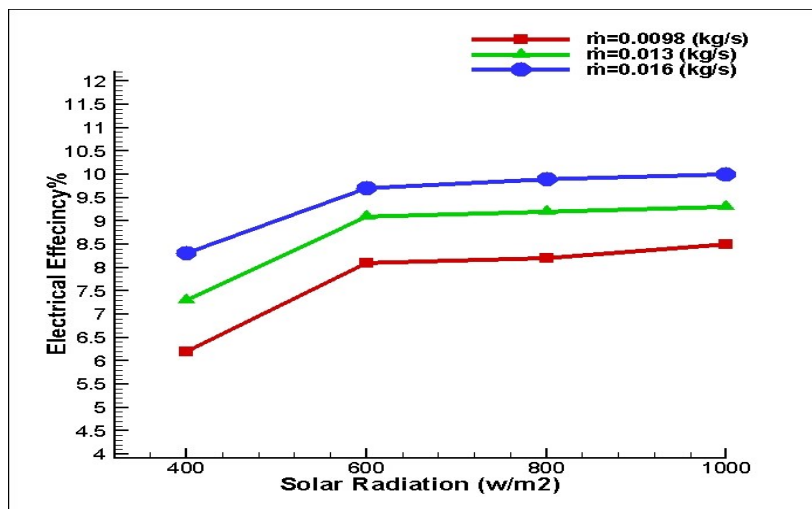


Figure 9: The variation of electrical efficiency in case 1 (fully covered with PV) at a different flow rate.

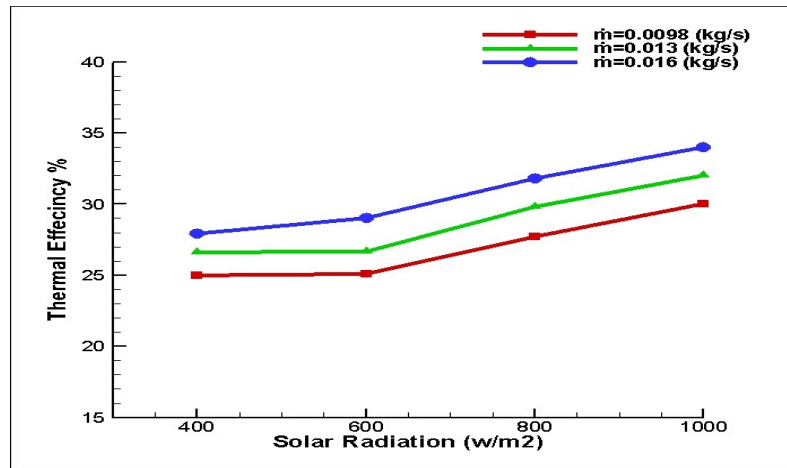


Figure 10: The variation of thermal efficiency in case 1 (fully covered with PV) at a different flow rate.

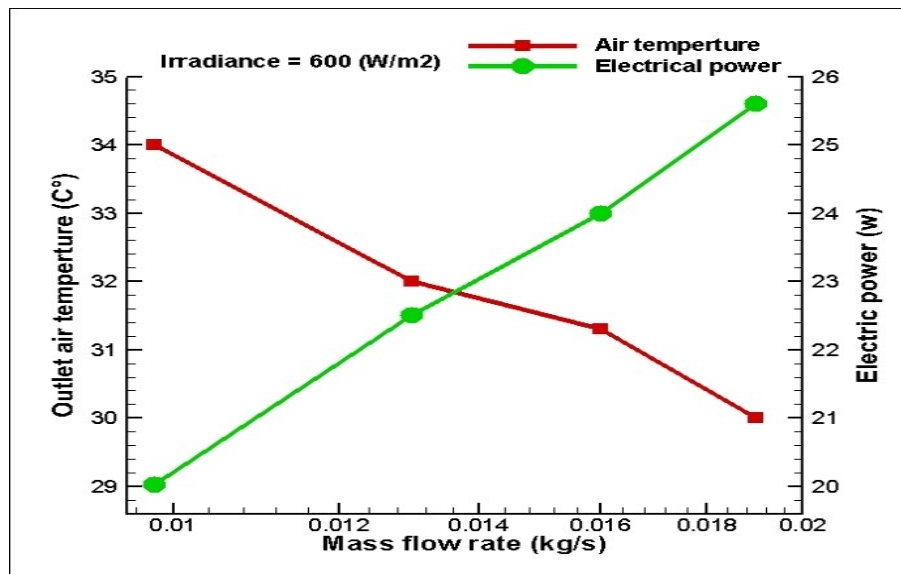


Figure 11: The electrical and thermal gain as a function of mass flow rate.

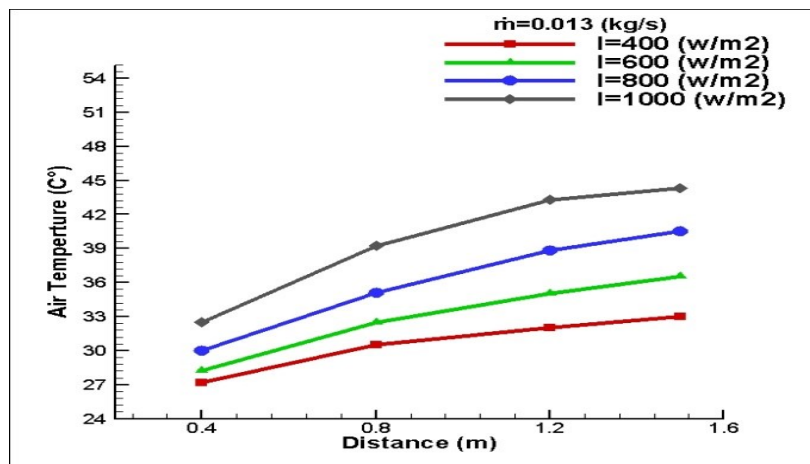


Figure 12: Experimentally air temperature variation along with the distance of the PV/T for (partially covered with PV) at a different solar radiation.

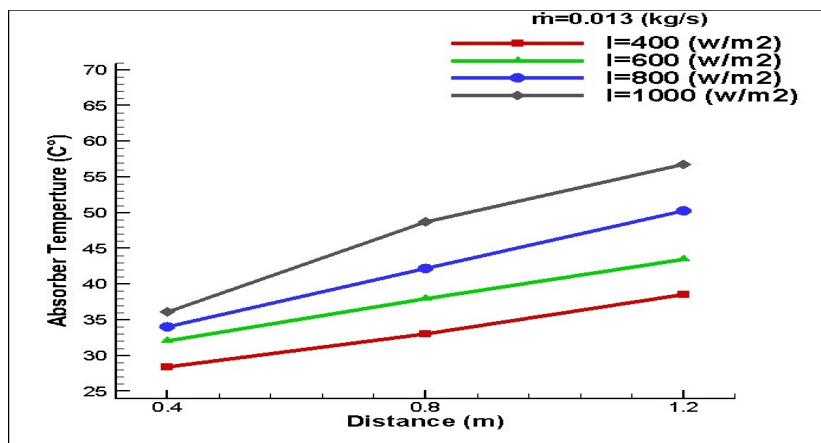


Figure 13: Experimental absorber temperature variation along with the distance of the PV/T collector for case 2 (partially covered with PV) at a different solar radiation.

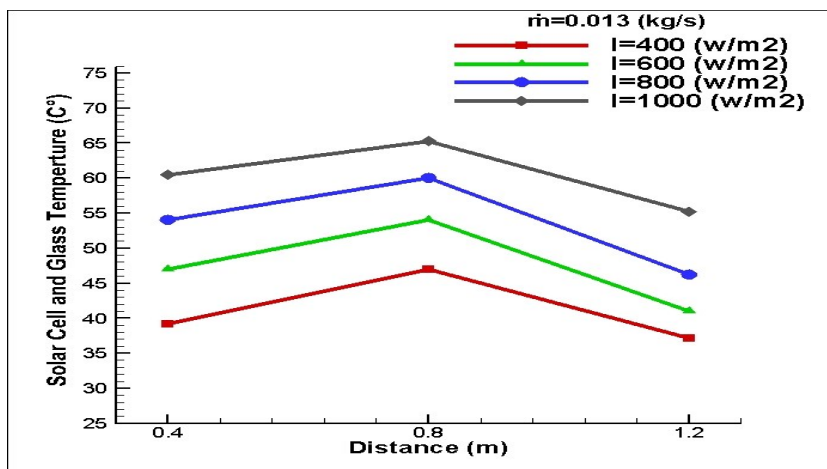


Figure 14: Experimentally PV cell and glass temperature variation along with the distance of the PV/T collector for case 2 (partially covered with PV) at a different solar radiation.

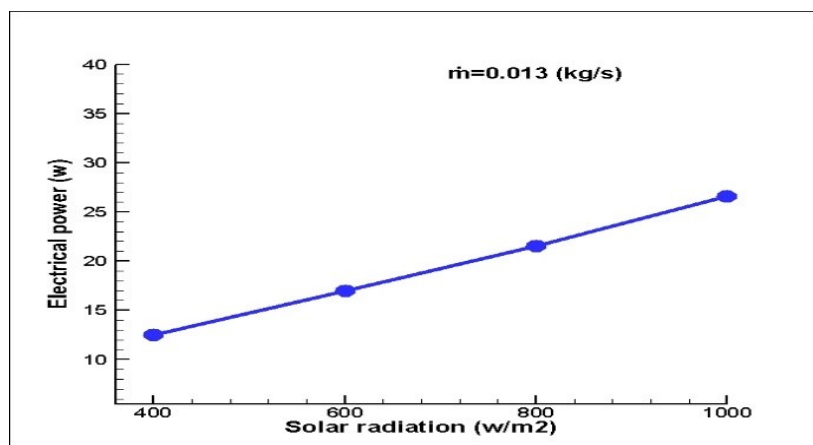


Figure 15: Variation of the electrical power generated with respect to solar radiation variation for case 2 (33% of PV/T collector covered with glass).

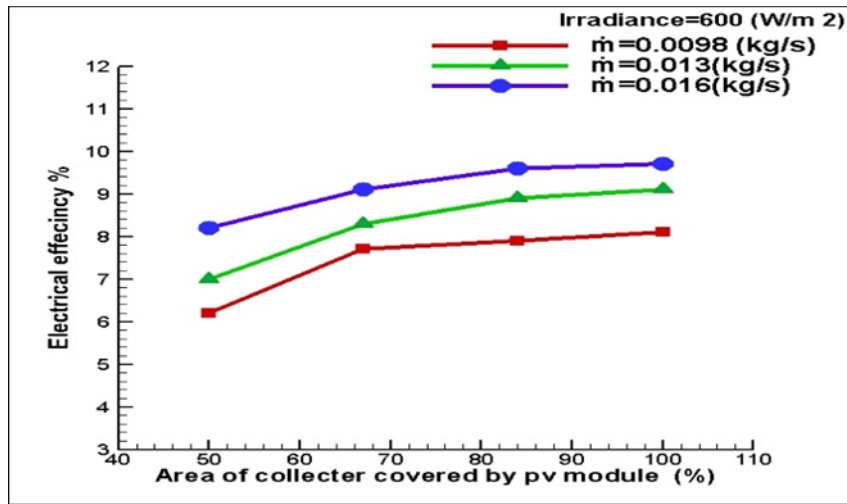


Figure 16: The variation of electrical efficiency with an area coverage rate of PV modules.

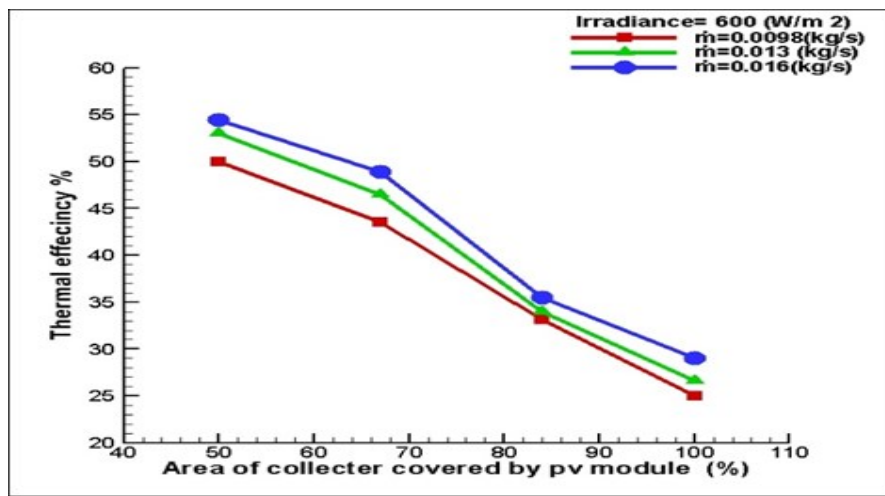


Figure 17: The variation of thermal efficiency with an area coverage rate of PV modules.

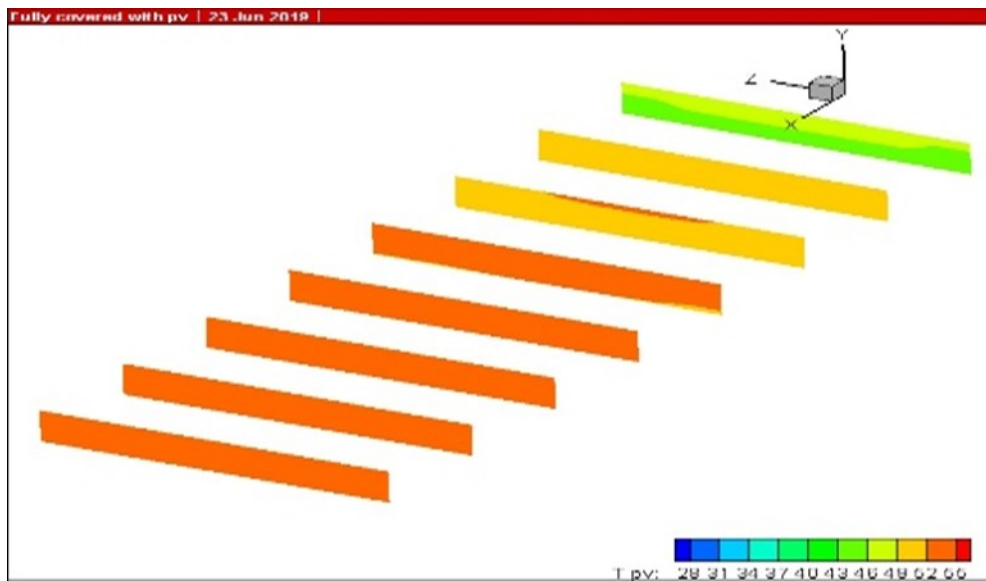


Figure 18: Isotherm contours of PV modules in the PV/T system for case 1 (fully covered with PV modules).

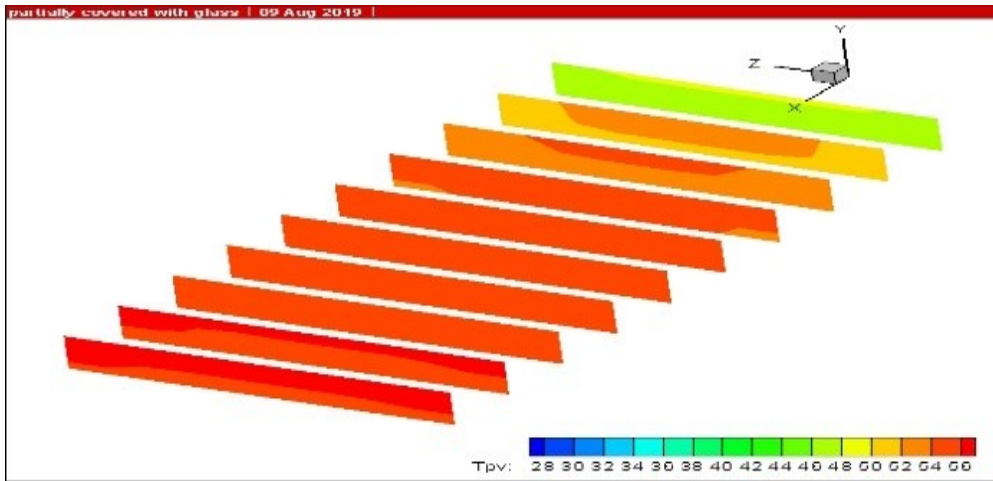


Figure 19: Isotherm contours of PV modules in the PV/T system for case 2 (partially covered with PV modules).

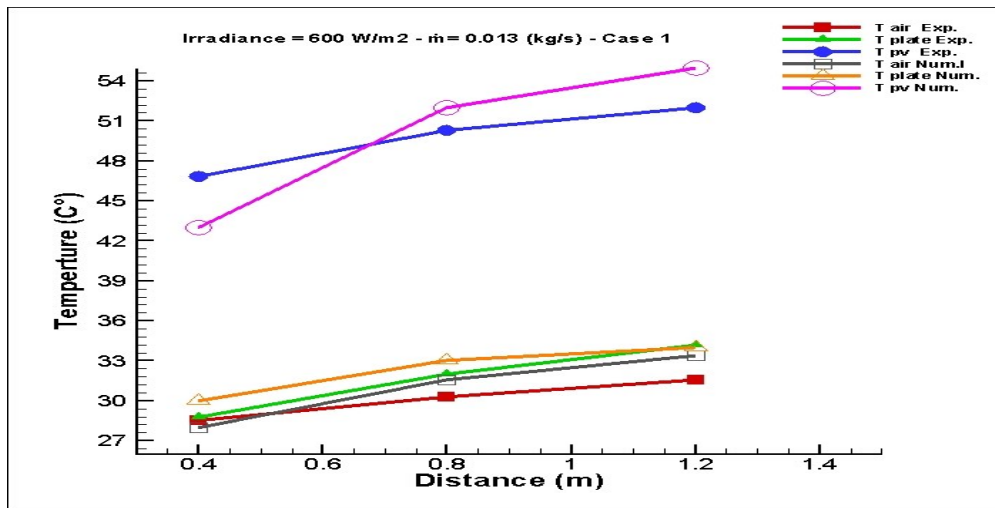


Figure 20: Comparison between experimental and numerical results for case 1 (fully covered with PV modules).

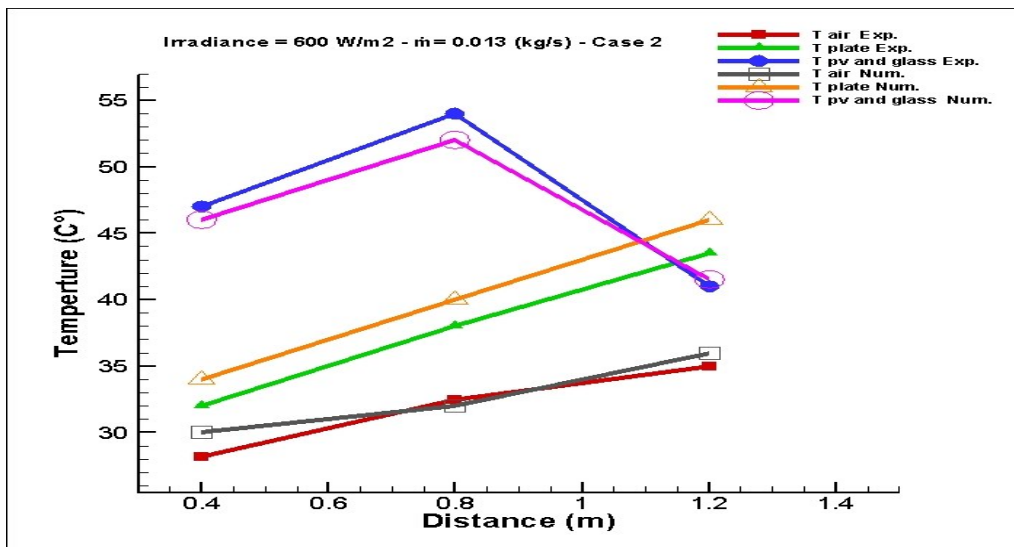


Figure 21: Comparison between experimental numerical results for case 2 (partially covered with PV modules).

## 6. Conclusions

On the basis of the study, the hybrid PV/T air collector with different configurations. The following points have been concluded:

- i. PV/T system fully covered with PV is gainful when the electrical generation is the primary requirement. While the PV/T system partially covered with glass performs better in the thermal generation.
- ii. The effect of increasing the glass area indicates that thermal efficiency increases also reach 55% when half of the PV/T collector covered with glass and 50% when one-third of the PV/T collector covered with glass.
- iii. Optimizing the electrical power and outlet air temperature with the mass flow rate advised to operate the PV/T collector at a moderate flow rate (0.013 kg/s) to obtain the required hot air and electrical power.
- iv. Optimizing the outlet air temperature and electrical power with area coverage rate by PV module conclude that, 33% of the PV/T collector covered with glass gives the best results in reaching the balance in the electrical and thermal gain.

## Symbols and units:

- A<sub>x</sub>: Area in the direction of east and west,  $m^2$ .  
 A<sub>y</sub>: Area in the direction of top and bottom,  $m^2$ .  
 A<sub>z</sub>: Area in the direction of north and south,  $m^2$ .  
 $h_{out}$ : External heat transfer coefficient,  $w/m^2K$ .  
 $h_{in}$ : Internal heat transfer coefficient,  $W/m^2.K$ .  
 I, j, k: Positions in the (x, y, z) direction.  
 $k_{ted}$ : Thermal conductivity of Tedlar,  $W/m.K$ .  
 $k_{sc}$ : Thermal conductivity of PV cell,  $W/m.K$ .  
 $k_g$ : Thermal conductivity of glass,  $W/m.K$ .  
 $T_{pv}$ : Temperature of the PV cells,  $^{\circ}C$ .  
 $T_{amb}$ : Temperature of ambient air,  $^{\circ}C$ .  
 $V_f$ : Air following velocity  $m/s$ .  
 $V_w$ : Wind velocity,  $m/s$ .  
 $\tau_g$ : Transmissivity of glass surface.  
 $\alpha_{pv}$ : PV modules absorptivity.  
 $\delta_{ted}$ : Thickness of Tedlar layer,  $m$ .  
 $\delta_{sc}$ : Thickness of PV cell  $m$ .  
 $\delta_g$ : Thickness of glass layer,  $m$ .  
 $\delta_{eva}$ : Thickness of EVA layer,  $m$ .

## References

- [1] D. Atheaya, A. Tiwari, G. Tiwari, and I. Al-Helal, "Analytical characteristic equation for partially covered photovoltaic thermal (pvt) compound parabolic concentrator (cpc)," *Solar Energy*, vol. 111, pp.176–185, 2015.
- [2] F. Yazdanifard, E. Ebrahimnia-Bajestan, and M. Ameri, "Investigating the performance of a water-based photovoltaic/thermal (pv/t) collector in laminar and turbulent flow regime," *Renewable Energy*, vol. 99, pp.295–306, 2016.
- [3] M. Tian, X. Yu, Y. Su, H. Zheng, and S. Riffat, "A study on incorporation of transpired solar collector in a novel multifunctional pv/thermal/daylighting (pv/t/d) panel," *Solar Energy*, vol. 165, pp.90–99, 2018.
- [4] M. Farshchimonfared, J. Bilbao, and A. Sproul, "Channel depth, air mass flow rate and air distribution duct diameter optimization of photovoltaic thermal (pv/t) air collectors linked to residential buildings," *Renewable energy*, vol. 76, pp. 27–35, 2015.
- [5] S. Bambrook and A. Sproul, "A solvable thermal circuit for modelling pvt air collectors," *Solar Energy*, vol. 138, pp. 77–87, 2016.
- [6] A. Shahsavari and M. Ameri, "Experimental investigation and modeling of a direct-coupled pv/t air collector," *Solar Energy*, vol. 84, no. 11, pp. 1938–1958, 2010.
- [7] F. Yazdanifard, E. Ebrahimnia-Bajestan, and M. Ameri, "Investigating the performance of a water-based photovoltaic/thermal (pv/t) collector in laminar and turbulent flow regime," *Renewable Energy*, vol. 99, pp. 295–306, 2016.

- [8] Wu, Shuang-Ying, Chen Chen, and Lan Xiao, "Heat transfer characteristics and performance evaluation of water-cooled PV/T system with cooling channel above PV panel," *Renewable Energy* vol. 125, pp.936-946, 2018.
- [9] G. Tiwari, J. Yadav, D. Singh, I. Al-Helal, and A. M. Abdel-Ghany, "Exergoeconomic and enviroeconomic analyses of partially covered photovoltaic flat plate collector active solar distillation system," *Desalination*, vol. 367, pp. 186–196, 2015.
- [10] S. Tiwari, J. Bhatti, G. Tiwari, and I. Al-Helal, "Thermal modelling of photovoltaic thermal (pvt) integrated greenhouse system for biogas heating," *Solar Energy*, vol. 136, pp. 639–649, 2016.
- [11] J. Tonui and Y. Tripanagnostopoulos, "Performance improvement of pv/t solar collectors with natural air flow operation," *Solar energy*, vol. 82, no. 1, pp. 1–12, 2008.
- [12] H. B. Awbi, "Ventilation of building," E & FN Spon, 1991.
- [13] J. P. Holman, "Heat transfer," McGraw-Hill, Tenth Edition, New York, 2010.
- [14] Tiwari G. N., "Solar energy: fundamentals, design, modelling and Applications," Alpha Science International, 1st Ed, 2002.
- [15] S. Kalogirou, "Solar energy engineering," Elsevier, First Edition, 2009
- [16] Dubey D., Solanki S.C. and Tiwari A., "Energy and exergy analysis of PV/T air collectors connected in series," *Energy and Buildings*, Vol.41, PP.863-870, 2009.
- [17] B. Widyolar, L. Jiang, and R. Winston, "Spectral beam splitting in hybrid pv/t parabolic trough systems for power generation," *Applied Energy*, vol. 209, pp. 236–250, 2018.
- [18] J. Allan, H. Pinder and Z. Dehouche, "Enhancing the thermal conductivity of ethylene-vinyl acetate(eva) in apho to voltaic thermal collector," *AIP Advances*, vol.6, no.3, p.035011, 2016.